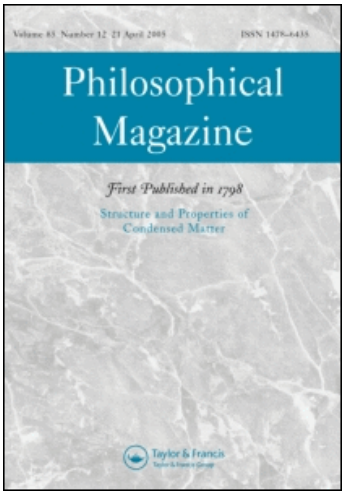

Philosophical Magazine
Publication details, including instructions for authors and subscription information:
http://www.informaworld.com/smpp/title~content=t713695589

Crystal plasticity model of shear and kink bands-energetic approach

Jan Kratochvíl[a]; Martin Kružík[ab]; Radan Sedláček[c]
[a] Department of Physics, Faculty of Civil Engineering, Czech Technical University, 166 29 Prague, Czech Republic [b] Institute of Information Theory and Automation of the ASCR, 182 08 Prague, Czech Republic [c] Lehrstuhl für Werkstoffkunde und Werkstoffmechanik, Fakultät für Maschinenwesen, Technische Universität München, 85747 Garching, Germany

First published on: 14 May 2010

To cite this Article Kratochvíl, Jan , Kružík, Martin and Sedláček, Radan(2010) 'Crystal plasticity model of shear and kink bands-energetic approach', Philosophical Magazine, 90: 27, 3729 — 3742, First published on: 14 May 2010 (iFirst)
To link to this Article: DOI: 10.1080/14786430903449411
URL: http://dx.doi.org/10.1080/14786430903449411

Philosophical Magazine
Vol. 90, Nos. 27–28, 21–28 September 2010, 3729–3742

Taylor & Francis
Taylor & Francis Group

Crystal plasticity model of shear and kink bands – energetic approach

Jan Kratochvíl[a], Martin Kružík[ab]* and Radan Sedláček[c†]

[a]*Department of Physics, Faculty of Civil Engineering, Czech Technical University, Thákurova 7, 166 29 Prague, Czech Republic;* [b]*Institute of Information Theory and Automation of the ASCR, Pod vodárenskou věží 4, 182 08 Prague, Czech Republic;* [c]*Lehrstuhl für Werkstoffkunde und Werkstoffmechanik, Fakultät für Maschinenwesen, Technische Universität München, Boltzmannstr. 15, 85747 Garching, Germany*

(*Received 4 June 2009; final version received 21 October 2009*)

We present a continuum crystal plasticity model of a lamellar deformation substructure of shear and kink bands. An evolutionary problem for the development of a spontaneous structural inhomogeneity is formulated in the framework of energetic solutions. Conti and Theil proved that in the case of an isothermal single-slip crystal, rigid plasticity with no hardening lamellaea form an optimal microstructure. Moreover, their model predicts the existence of a boundary layer which accommodates the lamellar substructure to displacement boundary conditions. It is suggested that the width of the shear and kink bands is a compromise: the minimization of bulk energy tends to decrease their size, while the energy of the band interfaces or the inner structure of the bands opposes this tendency.

Keywords: crystal plasticity; energetic approach; plastic deformation; plasticity of crystals

1. Introduction

Spontaneous structural inhomogeneity is the most distinguished mesoscopic feature of plastic deformation of ductile crystalline materials. The inhomogeneity is characterized by the formation of heterogeneous dislocation distributions such as tangles, veins, walls and cells, and localization of the plastic deformation in deformation bands. The evolution of deformation-induced long-range internal stresses and increasing lattice plane misorientation are characteristic features of the evolving dislocation pattern.

Detailed microscopic and X-ray observations on copper single crystals subjected to uniaxial tensile or cyclic deformation have been reviewed in the recent papers by Mughrabi et al. [1–3]. In the crystals oriented for single slip, early formed tangles in tension and veins in cycling consist mainly of edge dipolar loops. The loops are leftovers of glide dislocations partially annihilated by cross-slip. In later stages of cycling at a sufficiently high amplitude the deformation becomes localized into shear

*Corresponding author. Email: kruzik@utia.cas.cz
†Currently with AREVA NP, Erlangen, Germany

ISSN 1478–6435 print/ISSN 1478–6443 online

DOI: 10.1080/14786430903449411
http://www.informaworld.com

bands, called persistent slip bands (PSBs). PSBs are parallel to the slip plane and have a specific inner structure of walls and channels. The walls consist mainly of primary edge dipolar loops and serve as dislocation generation and annihilation centers. In the case of tension oriented for single slip the tangles are characteristic of the first stage of hardening. At the beginning of the second stage a secondary slip system is activated and a layer-like dislocation network of so-called grids (sheets) becomes one of the dominant dislocation patterns. The grids lie roughly parallel to the primary slip plane and consist of primary and secondary dislocations and their reaction products. As the shear deformation in the second stage is carried mainly by the primary dislocations, it can be treated as single slip.

The microstructures mentioned above are accompanied by kink bands oriented perpendicularly to the primary slip plane as seen in the scheme shown in Figure 1, which is a slight modification of the picture proposed by Mughrabi and Obst [1]. The kink walls have pronounced tilt misorientations around an axis that corresponds roughly to the line direction of the primary edge dislocations. The misorientation increases with deformation and reaches values less than 1°. The misorientations observed after cycling are always much smaller than those found after tensile deformation. The wavelength of the misorientation related to kink bands is an order of magnitude larger than the distances between the tangles, PSB walls or the widths of PSB and of the grid layers. These distances are typically of order μm on the other hand the kink walls have been found to be spaced between about 100 μm and 20 μm early and late in stage II of hardening [1]. In [3], p. 4047, Mughrabi states: 'in view of rather short dislocation glide paths in cyclic deformation, it is at present unclear how such subtle details with rather long-range periodicities develop in the dislocation pattern'. The observations raise other questions as well: Why are lamellar structures formed? What are the conditions of their formation? What determines their periodicity? In our opinion these questions can be answered, at least partly, within the framework of continuum crystal plasticity. The collective behavior of dislocations enters this framework trough hardening coefficients and through the inner structure of the lamellae and the energy of their boundaries.

The continuum model of a rate-independent, rigid-plastic crystal deformed by single slip is recalled in Section 2. As shown in Section 3 the energetic approach leads to the problem of the minimization of an energy functional subjected to boundary conditions and dissipation inequality. The minimization may result in spontaneous structural inhomogeneity. The exact mathematical proof of the existence of lamellar

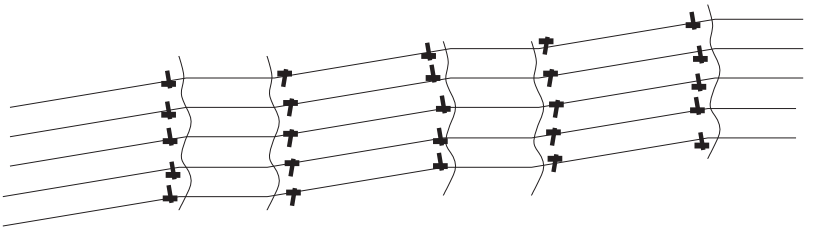

Figure 1. Scheme of shear and kink bands. A microphotograph of such structures can be found, e.g. in [1], Figure 4.

structures was given by Conti and Theil [4] for a single-slip rigid-plastic model with zero hardening, i.e. elastic deformation is reduced to lattice rotations and the hardening coefficient $h=0$. Moreover, they predicted the existence of a boundary layer which accommodates the lamellar structure to displacement boundary conditions. Their results indicate that the dominant effect, which causes formation of the lamellar structure, is the minimization of the dissipative energy (the rigidity excludes the elastic energy and $h=0$ causes no change of the dislocation stored energy). However, the rigid-plastic model exhibits an unwanted property: the lowest dissipative energy is reached for the lamellae of zero width. As indicated in the last section, the interface energy of the lamella boundaries or the energy needed to build an inner lamella structure suppress this tendency. The lamella structure periodicity is a compromise between these two tendencies.

2. Crystal plasticity

The crystal plasticity equations were introduced in classical papers, e.g. [5,6]. Here, the rigid-plastic approximation to the kinematics of isothermal crystal plasticity is considered. The constitutive assumption adopted in the present paper is a rate-independent single slip.

Each material point can be identified by its position in a reference configuration. The point which was at position $\boldsymbol{X}$ in the reference configuration is in the current configuration at time t in the position $\boldsymbol{x}(\boldsymbol{X},t)$. The difference $\boldsymbol{u}=\boldsymbol{x}-\boldsymbol{X}$ is the displacement of the material point $\boldsymbol{X}$. The deformation of the material is described by the transformation $\boldsymbol{F}$ of an infinitesimal material fiber from the reference to the current configuration,

$$\mathrm{d}\boldsymbol{x} = \boldsymbol{F}\,\mathrm{d}\boldsymbol{X}. \tag{1}$$

Assuming that $\boldsymbol{x}(\boldsymbol{X},t)$ is a continuous and differentiable vector field, this transformation can be introduced as the deformation gradient $\boldsymbol{F}=\partial\boldsymbol{x}/\partial\boldsymbol{X}=\boldsymbol{I}+\partial\boldsymbol{u}/\partial\boldsymbol{X}$, where $\boldsymbol{I}$ is the second-order identity tensor. In the rigid-plastic approximation the crystal lattice can (rigidly) rotate but it is not (elastically) strained. The plastic deformation of a crystal can be decomposed into two steps. First, the material flows through the crystal lattice by shearing along the active slip system to reach an intermediate configuration. This step is described by the plastic deformation gradient $\boldsymbol{F}^{\mathrm{p}}$, $\det\boldsymbol{F}^{\mathrm{p}}=1$. Second, the plastic deformation $\boldsymbol{F}^{\mathrm{p}}$ is followed by a rigid rotation $\boldsymbol{R}$ of the lattice representing the elastic part of the deformation gradient. The corresponding decomposition reads

$$\boldsymbol{F} = \boldsymbol{R}\boldsymbol{F}^{\mathrm{p}}, \tag{2}$$

hence, $\det\boldsymbol{F}=1$. The plastic deformation gradient $\boldsymbol{F}^{\mathrm{p}}$ transforms the reference configuration into the lattice (intermediate) configuration, $\boldsymbol{R}$ transforms the lattice configuration to the current configuration, and $\boldsymbol{F}$ transforms the reference configuration into the current configuration.

Unlike $\boldsymbol{F}$, the tensors $\boldsymbol{F}^{\mathrm{p}}$ and $\boldsymbol{R}$ do not generally correspond to the gradient of a vector field, i.e. they may be individually incompatible. In the case of inhomogeneous plastic deformation $\boldsymbol{F}^{\mathrm{p}}$, the lattice rotation $\boldsymbol{R}$ can re-establish the compatibility of the

overall material deformation. The density of geometrically necessary dislocations (GNDs) required for the material to be compatible can be characterized by the GND density tensor $\boldsymbol{\Lambda} = \boldsymbol{R}^{\mathrm{T}} \operatorname{curl}(\boldsymbol{R}^{\mathrm{T}})$; an overview and analysis of various measures of the GND density is given in [7].

The velocity $\boldsymbol{v}$ of a material point is given by the material time derivative of its position, $\boldsymbol{v}(\boldsymbol{x}, t) = \dot{\boldsymbol{x}}(\boldsymbol{X}, t)$. Now we perform the time derivative of Equation (1),

$$\mathrm{d}\dot{\boldsymbol{x}} = \dot{\boldsymbol{F}}\,\mathrm{d}\boldsymbol{X} = \frac{\partial \boldsymbol{v}(\boldsymbol{x}, t)}{\partial \boldsymbol{X}}\mathrm{d}\boldsymbol{X} = \frac{\partial \boldsymbol{v}}{\partial \boldsymbol{x}}\boldsymbol{F}\boldsymbol{F}^{-1}\mathrm{d}\boldsymbol{x} = \boldsymbol{L}\,\mathrm{d}\boldsymbol{x}, \tag{3}$$

where $\boldsymbol{L}(\boldsymbol{x}, t) = \dot{\boldsymbol{F}}\boldsymbol{F}^{-1} = \partial \boldsymbol{v}/\partial \boldsymbol{x}$ is the velocity gradient. Using Equation (2), the latter can be decomposed[1] as

$$\boldsymbol{L} = \boldsymbol{L}^{\mathrm{p}} + \dot{\boldsymbol{R}}\boldsymbol{R}^{T}, \tag{4}$$

where $\boldsymbol{L}^{\mathrm{p}}$ is the rate of plastic distortion in the current configuration and $\dot{\boldsymbol{R}}\boldsymbol{R}^{T}$ is the lattice spin.

The motion of glide dislocations carrying plastic flow takes place on a prescribed slip system. The slip system is defined in the lattice configuration by the orthonormal unit vectors $\boldsymbol{s}$ in the direction of slip and the normal to the slip plane $\boldsymbol{m}$, where $\boldsymbol{s} \cdot \boldsymbol{m} = 0$. In the lattice configuration the vectors $\boldsymbol{s}$ and $\boldsymbol{m}$ are constant, given by the crystallographic structure. The plastic flow manifests itself in the requirement that the evolution of $\boldsymbol{F}^{\mathrm{p}}$ be governed by the slip rate $\dot{\gamma}(\boldsymbol{X}, t)$ on the slip system via the flow rule

$$\dot{\boldsymbol{F}}^{\mathrm{p}} = \boldsymbol{L}^{\mathrm{p}}\boldsymbol{F}^{\mathrm{p}}, \quad \boldsymbol{L}^{\mathrm{p}} = \dot{\gamma}\boldsymbol{s} \otimes \boldsymbol{m}. \tag{5}$$

Assuming that $\boldsymbol{F}^{\mathrm{p}} = \boldsymbol{I}$ initially, the flow rule (5) and the identities $(\boldsymbol{s} \otimes \boldsymbol{m}) \cdot (\boldsymbol{m} \otimes \boldsymbol{s}) = 1$ and $(\boldsymbol{s} \otimes \boldsymbol{m}) \cdot (\boldsymbol{s} \otimes \boldsymbol{m}) = 0$ yield

$$\boldsymbol{F}^{\mathrm{p}} = \boldsymbol{I} + \gamma \boldsymbol{s} \otimes \boldsymbol{m}, \quad \gamma = 0 \quad \text{initially}. \tag{6}$$

Hence, the admissible deformation gradient $\boldsymbol{F}$ has to be of the form

$$\boldsymbol{F} = \boldsymbol{R}(\boldsymbol{I} + \gamma \boldsymbol{s} \otimes \boldsymbol{m}). \tag{7}$$

From the last equation it follows that

$$\gamma = (\boldsymbol{F}\boldsymbol{m}) \cdot (\boldsymbol{F}\boldsymbol{s}). \tag{8}$$

The slip γ in the slip system in the current configuration is driven by the resolved shear stress τ,

$$\tau = \boldsymbol{R}\boldsymbol{s} \cdot (\boldsymbol{T}\boldsymbol{R}\boldsymbol{m}), \tag{9}$$

where $\boldsymbol{T}$ is the Cauchy stress tensor and $\boldsymbol{R}\boldsymbol{s}$ and $\boldsymbol{R}\boldsymbol{m}$ represent the slip direction and the normal to the slip plane in the current configuration, which rotates rigidly with the lattice. In a quasi-static process with no body forces the stress $\boldsymbol{T}$ has to satisfy the equilibrium equation

$$\operatorname{div} \boldsymbol{T} = 0. \tag{10}$$

Within the present mechanical framework the second law of thermodynamics is reduced to the requirement that the plastic dissipation be non-negative,

$$\tau\dot{\gamma} \geq 0. \tag{11}$$

Constitutive relations of the rate-independent rigid-plastic material are represented by the yield condition,

$$\begin{aligned} &\dot{\gamma} > 0, \quad \text{only if } \tau = \tau_{\mathrm{y}}, \\ &\dot{\gamma} < 0, \quad \text{only if } \tau = -\tau_{\mathrm{y}}, \end{aligned} \tag{12}$$

if $|\tau| < \tau_{\mathrm{y}}$, the rate $\dot{\gamma} = 0$. The critical resolved shear stress $\tau_{\mathrm{y}}(\boldsymbol{x}, t) \geq 0$ represents local dissipative internal forces that oppose slip. In a rate-independent material, $\tau \leq \tau_{\mathrm{y}}$. The evolution equation for τ_{y} is

$$\dot{\tau}_{\mathrm{y}} = h|\dot{\gamma}|, \tag{13}$$

where the hardening coefficient h is taken as a material parameter. The hardening coefficient h is generally a function of variables which may themselves be controlled by evolution equations. In the present context it seems that such variables are τ_{y} and $\boldsymbol{\Lambda}$. A higher level of the resolved shear stress τ_{y} promotes dislocation annihilation, hence, it may decrease the value of the hardening coefficient h; arrangements of GNDs described by the density tensor $\boldsymbol{\Lambda}$ can serve as favorable centers of generation and annihilation of dislocations. However, in the next section the energetic formulation is analyzed for the case of zero hardening, $h = 0$, only.

3. Energetic formulation

The shearing of a rigid-plastic crystal deformed by single slip is treated as a plane strain problem; we employed the results derived for two-dimensional energetic models. For the energetic solution it is convenient to formulate a power balance for the considered crystal plasticity model in the reference configuration, see [8]. The quasi-static stress equilibrium (10) in the reference configuration is

$$\mathrm{Div}\, \boldsymbol{T}_{\mathrm{ref}} = 0, \tag{14}$$

where Div means divergence with respect to the position vector $\boldsymbol{X}$ in the reference configuration and in the rigid-plastic model $\boldsymbol{T}_{\mathrm{ref}} = \boldsymbol{T}\boldsymbol{F}^{-\mathrm{T}}$. Multiplying Equation (14) by the velocity $\boldsymbol{v}$ yields $\mathrm{Div}\, \boldsymbol{T}_{\mathrm{ref}} \cdot \boldsymbol{v} = 0 = \mathrm{Div}(\boldsymbol{T}_{\mathrm{ref}}\boldsymbol{v}) - \boldsymbol{T}_{\mathrm{ref}} \cdot \nabla \boldsymbol{v}$. Using the divergence theorem, the integration over the body Ω in the reference configuration with the boundary $\partial\Omega$ provides the power balance

$$\int_{\Omega} \boldsymbol{T}_{\mathrm{ref}} \cdot \dot{\boldsymbol{F}}\, \mathrm{d}V = \int_{\partial\Omega} \boldsymbol{T}_{\mathrm{ref}}\boldsymbol{n} \cdot \boldsymbol{v}\, \mathrm{d}A, \tag{15}$$

where $\boldsymbol{n}$ is the unit outer normal to $\partial\Omega$. From the kinematical relations (3)–(5) and the resolved shear stress (9) we get

$$\boldsymbol{T}_{\mathrm{ref}} \cdot \dot{\boldsymbol{F}} = \tau\dot{\gamma}. \tag{16}$$

From (15) and the latter equation the power balance can be expressed in the form

$$\int_\Omega \tau\dot{\gamma}\,\mathrm{d}V = \int_{\partial\Omega} \boldsymbol{T}_{\mathrm{ref}}\boldsymbol{n}\cdot\boldsymbol{v}\,\mathrm{d}A. \tag{17}$$

We assume that the velocity $\boldsymbol{v}=\boldsymbol{v}_0$ is prescribed on a part $\partial\Omega_v$ of the boundary and the stress $\boldsymbol{T}_{\mathrm{ref}}$ on the complementary part $\partial\Omega_T$.

Considering Equation (17) for the velocity $\boldsymbol{v}$ and the incremental velocity $\boldsymbol{v}+\delta\boldsymbol{v}$ which both obey the boundary condition on $\partial\Omega_v$, and subtracting these two equations, one gets a weak formulation of the boundary value problem

$$\int_\Omega \tau\delta\dot{\gamma}\,\mathrm{d}V - \int_{\partial\Omega_T} \boldsymbol{T}_{\mathrm{ref}}\boldsymbol{n}\cdot\delta\boldsymbol{v}\,\mathrm{d}A = 0. \tag{18}$$

The relation (18) can be understood as a condition for an extremum of an energy functional. If a displacement is prescribed on the whole boundary $\partial\Omega$ or if the complementary part $\partial\Omega_T$ is stress free, the surface integral in (18) disappears. Such boundary conditions are typical for standard strain controlled tensile and cycling experiments.

For the considered model the problem of the specification of the energy functional and a method of determination of its minimum represented by a lamellar structure has been analyzed in [4] under the restrictive assumption that the hardening coefficient in Equation (13) is $h=0$, i.e. there is no hardening, and the critical resolved shear stress $\tau_y>0$ is constant (the results obtained for the case $h\neq 0$ are commented on in the Remark at the end of this section). For $h=0$ and a zero surface integral the boundary value problem (18), where the yield condition (12) is incorporated, is reduced to

$$\int_\Omega \tau_y|\delta\dot{\gamma}|\mathrm{d}V = 0. \tag{19}$$

Now we recall the results of the analysis given in Conti and Theil [4]. They demonstrated rigorously that the model predicts the formation of a lamellar structure as the lowest energy microstructure formed. The mathematical proofs and the relevant references can be found in their paper [4]. For the energetic approach developed in a general context in [9,10], it is typical to formulate the minimization problem in an incremental way [4] by considering a discretization of the time interval $[0,T]$ of the deformation process, $0=t_0<t_1<t_2\cdots<t_N=T$. The minimization problem (19) is modified to: given the state $[\boldsymbol{x}(t_k),\gamma(t_k)]$ at time t_k we look for the position vector $\boldsymbol{x}$ and the slip strain γ at time t_{k+1}. These are found as a minimizer of the incremental functional

$$I_k(\boldsymbol{x},\gamma) = \int_\Omega \phi(\dot{\gamma}\ -\gamma(t_k),\boldsymbol{v},\gamma,\boldsymbol{x})\mathrm{d}V, \tag{20}$$

where the dissipation function ϕ is defined as

$$\phi(\dot{\gamma},\boldsymbol{v},\gamma,\boldsymbol{x}) = \begin{cases} \tau_{\mathrm{y}}|\dot{\gamma}| & \text{if } \boldsymbol{F}=\boldsymbol{R}(\boldsymbol{I}+\gamma\boldsymbol{s}\otimes\boldsymbol{m}), \\ +\infty & \text{otherwise,} \end{cases} \tag{21}$$

and τ_y is constant.

The infinity in formula (21) guarantees in a formal way that the lattice strain is negligible. The latter corresponds to the assumption that the elastic energy is infinite whenever the elastic part of the deformation gradient $\boldsymbol{F}$ is not a lattice rotation.

In summary, we are looking for a position vector field $\boldsymbol{x}(\boldsymbol{X}, t)$ of the body Ω which satisfies: (i) the kinematical rigid-plastic restriction $\nabla \boldsymbol{x} = \boldsymbol{R}(\boldsymbol{I} + \gamma \boldsymbol{s} \otimes \boldsymbol{m})$; (ii) the displacement boundary conditions at $\partial\Omega_v$; and (iii) it minimizes the incremental functional I_k. Due to (6) the time integration in (20) can be evaluated and the slip γ can be expressed through $\boldsymbol{F}$ using (8), hence, the problem can be implicitly formulated as the minimization in terms of the position vector field $\boldsymbol{x}$. As I_k can be explicitly constructed, the discretization (20) may be reduced to a single time interval $[t_0, t]$. Knowing $\boldsymbol{x}$ at time t_0 we denote its gradient $\boldsymbol{F}_0 = \nabla \boldsymbol{x}(t_0) = \boldsymbol{R}_0(\boldsymbol{I} + \gamma_0 \boldsymbol{s} \otimes \boldsymbol{m})$ for the rotation $\boldsymbol{R}_0 = \boldsymbol{R}(t_0)$ and slip $\gamma_0 = \gamma(t_0)$ and the incremental problem (20) and (21) then becomes

$$J(\boldsymbol{x}) = \int_\Omega W_{\mathrm{ep}}(\boldsymbol{F}; \boldsymbol{F}_0) \mathrm{d}V, \tag{22}$$

where W_{ep} is the energy density

$$W_{\mathrm{ep}}(\boldsymbol{F}; \boldsymbol{F}_0) = \begin{cases} \tau_{\mathrm{y}} |\gamma(\boldsymbol{F}) - \gamma(\boldsymbol{F}_0)| & \text{if } \boldsymbol{F} = \boldsymbol{R}(\boldsymbol{I} + \gamma \boldsymbol{s} \otimes \boldsymbol{m}), \\ +\infty & \text{otherwise.} \end{cases} \tag{23}$$

The main aim of the paper [4] was to study the minimization for (22) and (23). As noted by the authors in [4], the existence of a solution can only be expected for very special boundary conditions, i.e. affine boundary conditions (Dirichlet boundary conditions affinely depending on the positions of boundary points in the reference configuration) of the form $\boldsymbol{R}(\boldsymbol{I} + \gamma \boldsymbol{s} \otimes \boldsymbol{m})\boldsymbol{X}$; generally a compensating boundary layer is formed. The reason is that the discrete nature of the crystalline slip system makes the energy density W_{ep} not quasi-convex, which in turn favors the spontaneous formation of a microstructure. Typically, if affine boundary conditions are prescribed, the minimization of the energy functional $J(\boldsymbol{x})$ in (22) leads to highly oscillatory behavior of minimizing sequences and its minimum cannot be reached due to finer and finer oscillations of $\boldsymbol{F}$, cf. [11]. This may also happen if loading is applied to the specimen. This non-physical effect indicates that the proposed model, on which (22) and (23) are based, does not reflect correctly the observed phenomena (the observed shear and kink bands have a finite wavelength, and the energy of the banded crystal has a definite value). Moreover, from the microscopic point of view it is desirable to know the character of the oscillations; at a macroscopic level, boundary conditions imposed by the experimental setup have to be matched.

The mathematical study of the character of the oscillations and the problem of the boundary conditions is based on the concept of quasi-convexity (the effects controlling the refinement of the microstructure are discussed in the following section). In the constitutive assumption (23) the density W_{ep} is replaced by a quasi-convex envelope W^{qc}; the envelope W^{qc} is defined as the largest quasi-convex function which is less than or equal to W_{ep}, cf. Figure 2 (for a more detailed presentation of the concept of quasi-convexity see the Appendix). Minimization of $J(\boldsymbol{x})$ corresponds to the microstructure formed, and the minimizer of the functional

$J^{qc}(\boldsymbol{x})$ related to W^{qc} characterizes the average macroscopic properties of the microstructure. The relation between J and J^{qc} is demonstrated by a minimizing sequence [12]: for each $\boldsymbol{x}$, there is a sequence $\{\boldsymbol{x}_j\}$ converging weakly (in a suitable Sobolev space) to $\boldsymbol{x}$ such that

$$J^{qc}(\boldsymbol{x}) = \liminf_{j\to\infty} J(\boldsymbol{x}_j). \tag{24}$$

We refer to Figure 2 for W_{ep} and its quasi-convex envelope W^{qc}. A minimizing sequence $\{\boldsymbol{x}_j\}$ can be constructed in the following way. Roughly speaking, an imposed deformation gradient $\boldsymbol{F}$ such that $W_{ep}(\boldsymbol{F}, \boldsymbol{F}_k) = +\infty$ can be obtained as the 'average' of two rigid-plastic deformations $\boldsymbol{F}_1$ and $\boldsymbol{F}_2$ with finite energy and $\text{rank}(\boldsymbol{F}_1 - \boldsymbol{F}_2) = 1$, i.e. $\boldsymbol{F} = \mu\boldsymbol{F}_1 + (1-\mu)\boldsymbol{F}_2$ for some volume fraction $0 < \mu < 1$. The position vector field $\boldsymbol{x}_j(\boldsymbol{X})$ of the minimizing sequence is represented by a lamellar structure [4]

$$\boldsymbol{x}_j(\boldsymbol{X}) = (\mu\boldsymbol{F}_1 + (1-\mu)\boldsymbol{F}_2)\boldsymbol{X} + \boldsymbol{a}\frac{1}{j}\chi_\mu(j(n\cdot X + c)), \tag{25}$$

where $d := 1/j$ sets the scale of the lamellar structure. The vector $\boldsymbol{a}$ determines the direction of the structure amplitude and $\boldsymbol{n}$ is the unit normal to the lamellae; they are related through $\boldsymbol{F}_1 - \boldsymbol{F}_2 = \boldsymbol{a}\otimes\boldsymbol{n}$, c represents the phase relation between successive lamellae, and $\chi(\xi)$ is a continuous, periodic, piecewise-linear function of the argument $\xi = (\boldsymbol{n}\cdot\boldsymbol{X} + c)/d$ such that $\partial\chi_\mu/\partial\boldsymbol{X} - 1 = 1 - \mu$ for $\xi \in (0, \mu)$, and $\partial\chi_\mu/\partial\boldsymbol{X} - 1 = -\mu$ for $\xi \in (\mu, 1)$. Hence, to accommodate the deformation imposed by the

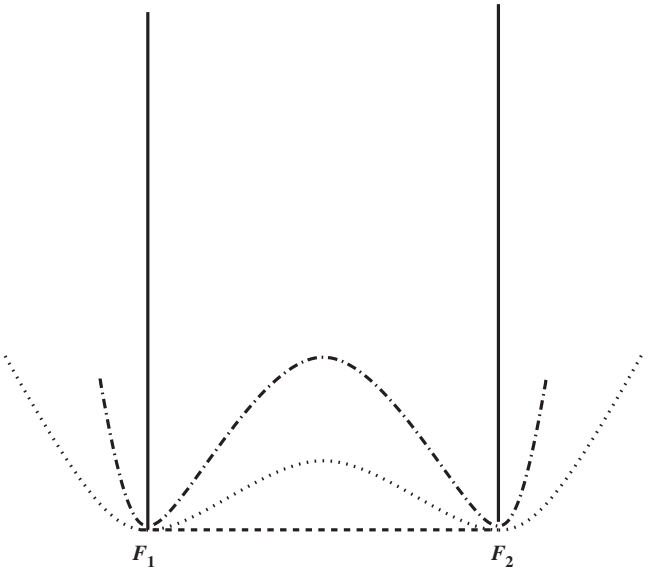

Figure 2. Non-quasi-convexity of W_{ep} between tensors $\boldsymbol{F}_1$, $\boldsymbol{F}_2$. W_{ep} can be seen as a limit of an elastoplastic energy density (dotted line) if elastic moduli tend to infinity (solid lines – considered case); the dashed-dotted line indicates increasing elastic moduli. The quasi-convex envelope W^{qc} of W_{ep} between $\boldsymbol{F}_1$ and $\boldsymbol{F}_2$ is depicted by the dashed line.

boundary conditions the system oscillates between two rigid-plastic deformations $\boldsymbol{F}_1$ and $\boldsymbol{F}_2$. Indeed, we see that

$$\nabla \boldsymbol{x}_j(X) = \mu \boldsymbol{F}_1 + (1-\mu)\boldsymbol{F}_2 + \chi'_\mu(j(n\cdot X + c))\boldsymbol{a}\otimes \boldsymbol{n}.$$

As $\boldsymbol{F}_1 - \boldsymbol{F}_2 = \boldsymbol{a}\otimes\boldsymbol{n}$ we get that $\nabla \boldsymbol{x}_d(\boldsymbol{X}) \in \{\boldsymbol{F}_1, \boldsymbol{F}_2\}$. Hence, if $W_{\mathrm{ep}}(\boldsymbol{F}_i, \boldsymbol{F}_0) < +\infty$ for $i = 1, 2$ then

$$W^{\mathrm{qc}}(\boldsymbol{F}, \boldsymbol{F}_0) \le \mu W_{\mathrm{ep}}(\boldsymbol{F}_1, \boldsymbol{F}_0) + (1-\mu) W_{\mathrm{ep}}(\boldsymbol{F}_2, \boldsymbol{F}_0) < +\infty.$$

Conti and Theil [4] proved that if we prescribe affine boundary conditions on the boundary of the domain, i.e. $\boldsymbol{x}(\boldsymbol{X}) = \boldsymbol{F}\boldsymbol{X}$ for $\boldsymbol{X} \in \partial\Omega$, then the deformation given by (25) is a minimizing sequence if a suitable modification is introduced in the vicinity of $\partial\Omega$. They showed that the magnitude of the energy contribution of this modification is bounded by a constant times $d := 1/j$, i.e. it vanishes if the period of the oscillations decreases. This construction is a main ingredient in their proof that the quasi-convex envelope W^{qc} can be reached by laminated microstructures. In general, following relaxation theory of the calculus of variations, replacing W_{ep} in formula (22) by the quasi-convex envelope W^{qc} (see Figure 2) sets up a minimization problem which possesses a minimizer and describes the limiting behavior of the oscillations if their length-scale d tends to zero [11]. While the computations of the quasi-convex envelope always involve affine boundary conditions we may face the non-existence of a solution to the original problem (23) even if the problem is equipped with loading by external forces. Namely, given the external forces we solve the relaxed problem with W^{qc} instead of W_{ep}. This gives us a deformation field $\boldsymbol{x}$ defined for almost all $\boldsymbol{X}$ in Ω. Hence, we then look at $\boldsymbol{F} = \nabla \boldsymbol{x}(\boldsymbol{X})$ for a fixed $\boldsymbol{X}$ and find out the microstructure corresponding to $\boldsymbol{F}$. By the result of [4] it is a lamellar structure. Thus, we get *a posteriori* a microscopic plastic deformation localized around $\boldsymbol{X}$. This is even more pronounced if we consider a finite element approximation of the relaxed problem using element-wise affine deformations. Then the gradient of $\boldsymbol{x}$ is element-wise constant, so there is a simple laminated microstructure corresponding to $\nabla \boldsymbol{x}$ on every element; see Figure 3. As the deformation must be globally continuous we have to match boundary conditions over element boundaries as in Figures 4 and 5.

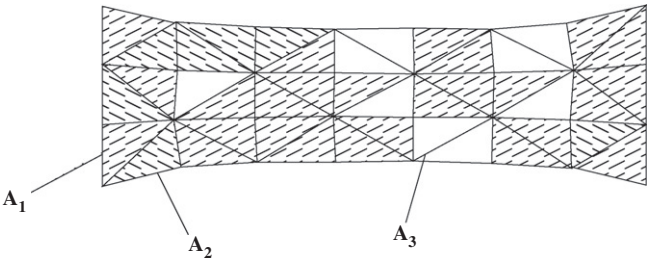

Figure 3. A specimen with a triangular mesh and $\nabla \boldsymbol{x}$ taking values $\boldsymbol{A}_1$, $\boldsymbol{A}_2$, and $\boldsymbol{A}_3$. On some elements the microstructure must match affine boundary conditions $\boldsymbol{x}(\boldsymbol{X}) = \boldsymbol{A}_1\boldsymbol{X}$, or $\boldsymbol{x}(\boldsymbol{X}) = \boldsymbol{A}_2\boldsymbol{X}$ for X from the element boundary. This creates an energy contribution which vanishes with the increasing finesse of laminates. In general, there may also be a part of the specimen where no microstructure appears. These regions are denoted $\boldsymbol{A}_3$.

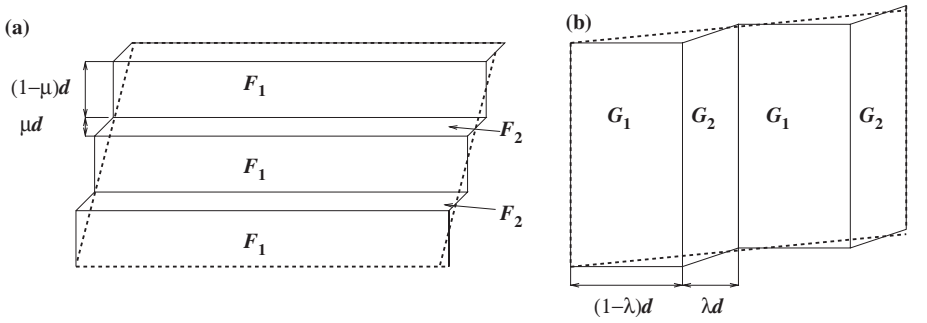

Figure 4. Shear (a) and kink band (b) lamellae with finite periodicity. Each construction matches affine displacement boundary conditions on two opposite sides. However, refining this construction leads to lower energies. In the limit for $d \to 0$, the periodicity of lamellar structure tends to zero. Here $\mathrm{rank}(\boldsymbol{F}_1 - \boldsymbol{F}_2) = \mathrm{rank}(\boldsymbol{G}_1 - \boldsymbol{G}_2) = 1$.

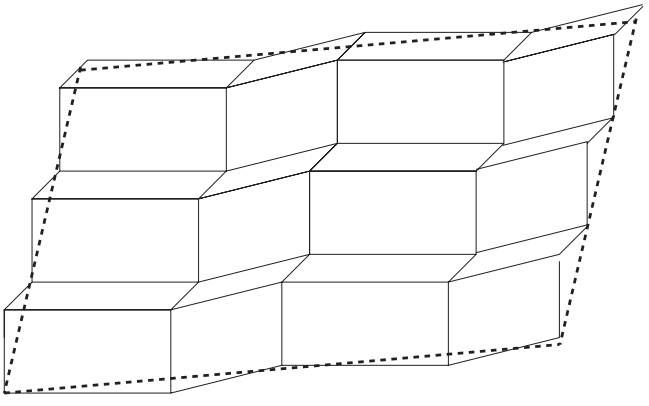

Figure 5. Composition of two basic constructions from Figure 4. The dashed line denotes the macroscopic deformation.

The case of shear bands is shown schematically in Figure 4a. The periodicity of the lamellar structure is d. Analogically, Figure 4b illustrates kink bands where $\boldsymbol{G}_i$, $i = 1, 2$, are corresponding deformation gradients and λ is the volume fraction.

Moreover, as shown in [4], the optimal microstructure is a lamellar structure with $\boldsymbol{F}$ alternating between $\boldsymbol{F}_1 := \boldsymbol{F} - (1-\mu) a \otimes b$ where $\boldsymbol{F}_2 := \boldsymbol{F} + \mu a \otimes b$, where a unit vector b is a solution (up to the sign) of $|\boldsymbol{F} b^{\perp}| = 1$, and $a = \boldsymbol{F} b^{\perp}$ ($b^{\perp}$ denotes a vector perpendicular to b). Here $\boldsymbol{F}$ denotes the average deformation gradient determined by boundary conditions. Consider the following situation.

Let $\boldsymbol{s} = (-1, 1)/\sqrt{2}$ and $\boldsymbol{m} = (-1, -1)/\sqrt{2}$. Let, further, $2 > \gamma > 0$ be given and consider a simple shear macroscopic deformation given by $\boldsymbol{x}(\boldsymbol{X}) = \boldsymbol{F}\boldsymbol{X}$, where

$$\boldsymbol{F} = \begin{pmatrix} 1 & 2-\gamma \\ 0 & 1 \end{pmatrix}. \tag{26}$$

Then $\boldsymbol{F}=\gamma/2\boldsymbol{I}+(1-\gamma/2)\boldsymbol{F}_2$, where

$$\boldsymbol{F}_2=\begin{pmatrix}1 & 2\\ 0 & 1\end{pmatrix}. \tag{27}$$

Notice that $\boldsymbol{F}_2=\boldsymbol{R}(\boldsymbol{I}-2\boldsymbol{s}\otimes\boldsymbol{m})$ and that $\boldsymbol{F}_2-\boldsymbol{I}=2\boldsymbol{a}\otimes\boldsymbol{b}$ where $\boldsymbol{a}=(-1,0)$ and $\boldsymbol{b}=(0,1)$. A simple calculation shows that

$$\boldsymbol{R}=\begin{pmatrix}0 & 1\\ -1 & 0\end{pmatrix}. \tag{28}$$

Now, if we put $\mu:=\gamma/2$ we have $\boldsymbol{F}=\mu\boldsymbol{I}+(1-\mu)\boldsymbol{R}(\boldsymbol{I}-2\boldsymbol{s}\otimes\boldsymbol{m})$; then $W^{\mathrm{qc}}(\boldsymbol{F}_0,\boldsymbol{F})<+\infty$, if $\det\boldsymbol{F}_0=1$ and $|\boldsymbol{F}\boldsymbol{s}|\leq 1$. Similarly, for some $0<\lambda<1$ put $\boldsymbol{F}^{\top}=:\boldsymbol{G}=\lambda\boldsymbol{I}+(1-\lambda)\tilde{\boldsymbol{R}}(\boldsymbol{I}+\tilde{\gamma}\boldsymbol{s}\otimes\boldsymbol{m})$ representing a kink macroscopic deformation ($\tilde{\boldsymbol{R}}$ is a rotation, $\tilde{\gamma}>0$). Then again $W^{\mathrm{qc}}(\boldsymbol{F}_0,\ \boldsymbol{G})<+\infty$. The construction of microstructures arising from shear and kink bands is depicted in Figure 4 for $\boldsymbol{F}_1=\boldsymbol{G}_1:=\boldsymbol{I}$, $\boldsymbol{F}_2:=\boldsymbol{R}(\boldsymbol{I}-2\gamma\boldsymbol{s}\otimes\boldsymbol{m})$, and $\boldsymbol{G}_2:=\tilde{\boldsymbol{R}}(\boldsymbol{I}+\gamma\boldsymbol{s}\otimes\boldsymbol{m})$. The numbers $1-\lambda$ and $1-\mu$ represent volume fractions of the undeformed material.

These two basic constructions can be composed into the structure depicted in Figure 5.

Remark 3.1: In the case of elastoplastic crystals where W_{ep} is finite and contains the hardening term $c\tau_{\mathrm{y}}^2$ with some $c>0$ and if $h>0$ in Equation (13) then this hardening term has a convexifying effect on the energy [13]. Indeed, notice that at the time t_2, $\tau_{\mathrm{y}2}^2=(\tau_{\mathrm{y}1}+h|\gamma_2-\gamma_1|)^2$, where the quantities with sub-index 1 refer to the previous time instant t_1. Hence, we can rewrite the hardening term as a convex function of γ_2. Thus, $h>0$ may prevent the formation of microstructures for larger time intervals. At the same time softening ($h<0$) may cause the creation of microstructures for large times even if there is no microstructure at the beginning. Here it is crucial that we include elastic energy. In the rigid-plastic approximation, however, the hardening has no convexifying effect on the total energy because it is finite only on a non-convex set. The same happens for softening, i.e. $h<0$.

4. Discussion

We proposed a mathematically rigorous way to explain the formation of lamellar microstructures in continuum, rate-independent, single-crystal plasticity restricted by the assumptions of elastic rigidity and zero hardening. The principal results of the previous section are symbolically expressed in Figure 5 which is a model representation of the schema from Figure 1 deduced from experiments. There, the shear strain is carried by the shear bands and the kink bands adjust the crystal lattice orientation on average to the applied shear. Our model does not introduce any length-scale into the problem. Namely, as already mentioned before, finer and finer lamellae decrease the bulk energy and displacement. Nevertheless, boundary conditions bring an additional energy contribution which vanishes with the thickness of the lamellae, $d\to 0$. However, the observations mentioned in the introduction show that the bands have a well-defined finite width. The reason is that the model neglects the energy needed to build interface boundaries or the inner structure of

the bands. In that the shear bands and the kink bands are very different. This probably provides an answer to the question posed by Mughrabi [3] and recalled in the introduction.

In the case of the kink bands the rotation $\boldsymbol{R}$ jumps across the kink boundaries and, hence, the GND density is non-zero there and is arranged in the dislocation boundaries. According to the classical paper by Read and Shockley [14] the interface energy per unit area for low-angle boundaries is approximately $[Gp/4\pi(1-\nu)]$ $\vartheta[A-\ln\vartheta]$, where G is the shear modulus, p the lattice parameter, ν Poisson's ratio, and A was estimated to be 0.23. ϑ is the relative rotation across the boundary in the scheme of Figure 5 and represents the density of geometrically necessary dislocations (GND) forming the boundary. In the present context ϑ can be understood as the GND density tensor $\boldsymbol{\Lambda}=\boldsymbol{R}^{\mathrm{T}}\,\mathrm{curl}(\boldsymbol{R}^{\mathrm{T}})$ introduced in Section 2. We may include the classical interfacial energy term in our model (23). A simple way would be to penalize spatial changes in the deformation gradient. The incremental problem corresponding to (22) then becomes

$$J_k(\boldsymbol{x})=\int_\Omega \left\{W_{\mathrm{ep}}(\nabla\boldsymbol{x};\boldsymbol{F}_0)+W_{int}(\boldsymbol{\Lambda})\right\}\mathrm{d}V, \tag{29}$$

where

$$W_{int}(\boldsymbol{\Lambda})=\begin{cases}[Gp/4\pi(1-\nu)]|\boldsymbol{\Lambda}|[A-\ln|\boldsymbol{\Lambda}|] & \text{if } |\boldsymbol{\Lambda}|>0 \text{ and } \boldsymbol{x}(x)=\boldsymbol{R}(x)(\boldsymbol{I}+\gamma(x)\boldsymbol{s}\otimes\boldsymbol{m}),\\ 0 & \text{otherwise.}\end{cases}$$

However, this interfacial energy still does not have to guarantee the existence of a solution due to the lack of full information about $\nabla\gamma$.

Another simple way would be to penalize spatial changes in the deformation gradient in the incremental problem corresponding to (22), for instance as,

$$J_k(\boldsymbol{x})=\int_\Omega \{W_{\mathrm{ep}}(\nabla\boldsymbol{x};\boldsymbol{F}_0)+\alpha|\nabla^2\boldsymbol{x}|^2\}\mathrm{d}V, \tag{30}$$

where $\nabla\boldsymbol{x}=\boldsymbol{R}(\boldsymbol{I}+\gamma\boldsymbol{s}\otimes\boldsymbol{m})$, $\boldsymbol{x}(\boldsymbol{X})=\boldsymbol{F}\boldsymbol{X}$ for some $\boldsymbol{F}$ with the unit determinant and $|\boldsymbol{F}\boldsymbol{s}|<1$ on the boundary, and $\alpha>0$. The main feature of this model of the interfacial energy is that a solution exists in the appropriate Sobolev space despite the fact that W_{ep} is not quasi-convex. The reason is that the first gradient of a minimizing sequence converges strongly and W_{ep} is lower semi-continuous. Thus, any solution inevitably has a finite number of smooth interfaces whose number decreases as α grows. This reflects two competing mechanisms in the problem. The increasing number of interfaces decreases the W_{ep} term in (29) while it makes the other term grow. We refer to [12] for another approach to include interfacial energy in the case of deformation theory of plasticity with a double-slip system. Another attempt to introduce an interfacial energy into the energy minimization problem was undertaken in [15] in the case of dislocation cell formation in a symmetric double slip.

The mechanism controlling the thickness of the shear bands is very different. In the case of shear bands the rotation is $\boldsymbol{R}=\boldsymbol{I}$, and the GNDs are not formed. However, there is a need for an energy to build the inner structure of the shear bands. The problem of the relation of the inner structure to the thickness of the shear band lamellae and their density was studied in [16,17]. The study concerned mature

persistent slip bands (PSBs) occurring in cyclically deformed metal single crystals (to our knowledge, analogous studies for sheet structures have not yet been done). The wavelength of their spontaneously formed ladder structure of dipolar dislocation walls and channels represents an intrinsic scale. The thickness of the PSB lamellae is controlled by inhomogeneous internal stresses created by the ladder structure of the bands. The applied cyclic shear strain with a given amplitude could be carried equally by a higher density of thinner PSBs or by a lower density of thicker PSBs. The energy of the internal stress of a PSB can be divided into the part within the PSB lamella and the part in the neighboring matrix structure. If each PSB of a certain thickness is split, e.g. into two PSBs, the volume of the PSB lamellae is the same and the energy in the lamellae decreases due to smaller thickness. The reason is that the normal stress component in the direction perpendicular to the PSBs increases with the square of the lamella thickness. On the other hand, the energy of the parts of the matrix neighboring to the PSBs increases as their total volume is doubled by the splitting. The explanation is that the internal stress energy of these parts per unit volume is nearly the same. It depends mainly on the shear stress component which is not influenced by the lamella splitting. Hence, the energy density increases to infinity when the thickness approaches zero. In the opposite limit of an infinite thickness the energy density also reaches infinity due to the increase of the internal stress in the thicker PSB lamellae. The observed thickness is a compromise between these two tendencies. The detailed computation confirming the above conclusion is given in [16,17]. However, to incorporate the internal structure mechanism in the current models of crystal plasticity and their energetic solution is a challenging problem and requires further research.

Acknowledgements

This work was supported by the grants VZ6840770021 (MŠMT ČR) and A100750802 (GAAV ČR).

Note

1. In detail: $\boldsymbol{L} = \dot{\boldsymbol{F}}\boldsymbol{F}^{-1} = \boldsymbol{R}\dot{\boldsymbol{F}}^{\mathrm{p}}(\boldsymbol{F}^{\mathrm{p}})^{-1}\boldsymbol{R}^{T} + \dot{\boldsymbol{R}}\boldsymbol{R}^{T}$, where $\dot{\boldsymbol{F}}^{\mathrm{p}}(\boldsymbol{F}^{\mathrm{p}})^{-1}$ is the rate of plastic distortion in the reference lattice, $\boldsymbol{R}\dot{\boldsymbol{F}}^{\mathrm{p}}(\boldsymbol{F}^{\mathrm{p}})^{-1}\boldsymbol{R}^{T} = \boldsymbol{L}^{\mathrm{p}}$ is the rate of plastic distortion rotated with the lattice into the current configuration, and $\dot{\boldsymbol{R}}\boldsymbol{R}^{T}$ is the lattice spin.

References

[1] H. Mughrabi and B. Obst, Z. Metallkunde 96 (2005) p.686.
[2] H. Mughrabi, Acta Materialia 54 (2006) p.3417.
[3] H. Mughrabi, Phil. Mag. 86 (2006) p.4037.
[4] S. Conti and F. Theil, Arch. Ration. Mech. Anal. 178 (2005) p.125.
[5] R.J. Asaro, Adv. Appl. Mech. 23 (1983) p.1.
[6] S.V. Harren, H.E. Dève and R.J. Asaro, Acta Metallurgica 36 (1988) p.2435.
[7] P. Cermelli and M. Gurtin, J. Mech. Phys. Solids 48 (2000) p.989.
[8] M. Gurtin, J. Mech. Phys. Solids 50 (2002) p.5.
[9] A. Mielke, F. Theil and V.I. Levitas, Arch. Ration. Mech. Anal. 162 (2002) p.137.

[10] A. Mielke and F. Theil, Nonlinear Differ. Equ. Appl. 11 (2004) p.151.
[11] B. Dacorogna, *Direct Methods in the Calculus of Variations*, Applied Mathematical Sciences, 2nd ed., Vol. 78, Springer, Berlin, 2008.
[12] S. Conti and M. Ortiz, Arch. Ration. Mech. Anal. 176 (2005) p.103.
[13] C. Carstensen, K. Hackl and A. Mielke, Proc. Royal Soc. London A 458 (2002) p.299.
[14] W.T. Read and W. Shockley, Phys. Rev. 78 (1950) p.275.
[15] J. Kratochvíl, M. Kružík and R. Sedláček, Phys. Rev. B 75 (2007) p.064104.
[16] V. Gregor and J. Kratochvíl, Internat. J. Plastic. 14 (1998) p.159.
[17] V. Gregor, J. Kratochvíl and M. Saxlová, *Width and density of persistent slip bands as a consequence of deformation mesostructure*, in *EUROMECH – MECAMAT on Mechanics of Materials with Instrinsic Length Scale*, Magdeburg, Germany, February 23–26, 1998, A. Bertram and F. Sidoroff, eds., Otto-von-Guericke University, Magdeburg, 1998, p.174.

Appendix. Quasi-convex functions

Consider a function $f:\mathbb{R}^{d\times d}\to\mathbb{R}\cup\{+\infty\}$. We say that f is quasi-convex if for a smooth bounded domain $O\subset\mathbb{R}^d$ it holds that for every $\phi\in C_0^\infty(O;\mathbb{R}^d)$ and all $A\in\mathbb{R}^{d\times d}$ ($|O|$ denotes the Lebesgue measure of O)

$$f(A)|O|\le\int_O f(A+\nabla\phi(\xi))\mathrm{d}\xi. \tag{31}$$

If $0\le f(A)\le C(1+|A|^p)$ for some $C>0$ then quasi-convexity is necessary and sufficient for weak lower semi-continuity of the functional $I(u)=\int_\Omega f(\nabla u(\xi))\mathrm{d}\xi$ defined for $u\in W^{1,p}(\Omega;\mathbb{R}^d)$. Here $W^{1,p}(\Omega;\mathbb{R}^d)$ is the space of functions integrable together with their gradient to the p-th power. The weak lower semi-continuity is a key ingredient when one proves the existence of a minimizer to I. If f is not quasi-convex we define its quasi-convexification as

$$\bar{f}(A):=\inf_{\phi\in C_0^\infty(O;\mathbb{R}^d)}=\frac{1}{|O|}\int_O f(A+\nabla\phi(\xi))\mathrm{d}\xi.$$

Lack of quasi-convexity typically brings finer and finer oscillations to the minimizing sequence of I. Replacing f by $\bar{f}$ in the definition of I defines the so-called relaxed problem which is mathematically well-posed and correctly describes macroscopic physical quantities. This the reason why we look for the quasi-convex envelope of the (microscopic) energy density.

Quasi-convexity is very difficult to verify, in general. However, convex functions are quasi-convex and it is also known that quasi-convex functions are convex along lines with points which differ by a rank-1 matrix. That is why laminates, i.e. constructions with piecewise affine deformations with rank-1 jumps in the gradients, are used to approximate the quasi-convex envelope. Nevertheless, quasi-convexity is a much weaker condition than convexity. We refer, e.g. to [11] for more details.